Vol 16 No 10, October 2007
1009-1963/2007/16(10)/2957-05
Chinese Physics
© 2007 Chin. Phys. Soc.
and IOP Publishing Ltd

Control of photoassociation reaction F+H→HF with ultrashort laser pulse*

Liu Li(刘 俐), Niu Ying-Yu(牛英煜),
Yuan Kai-Jun(元凯军), and Cong Shu-Lin(丛书林)†

Department of Physics, Dalian University of Technology, Dalian 116024, *China*

(Received 26 December 2006; revised manuscript received 11 January 2007)

The laser-induced vibrational state-selectivity of product HF in photoassociation reaction H+F→HF is theoretically investigated by using the time-dependent quantum wave packet method. The population transfer process from the continuum state down to the bound vibrational states can be controlled by the driving laser. The effects of laser pulse parameters and the initial momentum of the two collision atoms on the vibrational population of the product HF are discussed in detail. Photodissociation accompanied with the photoassociation process is also described.

Keywords: ultrashort laser pulse, photoassociation reaction, vibrational state-selectivity
PACC: 3450R, 8230N, 8240J

1. Introduction

With the development of the ultrashort pulse laser techniques, many new phenomena of laser–molecule interaction have been observed and investigated,[1−16] such as ac-Stark shift,[1,2] multiphoton ionization,[3−5] laser-induced continuum structure[6−8] and photoassociation reaction.[9−13] The photoassociation dynamics induced by laser pulse has been studied both experimentally and theoretically.[17−28] Marvet and Dantus investigated experimentally the formation of Hg_2 molecule with ultrashort laser pulse.[17] Javanainen and Matt described free–bound–bound photoassociation using the quasicontinuum approach.[21,22] Korolkov *et al* studied the photoassociation reaction induced by laser pulse with optimal parameters.[23−28]

In the present work, the photoassociation reaction F+H→HF steered by ultrashort laser pulse is theoretically studied by employing the quantum wave packet method. The relationship between the population, the laser pulse parameters and the initial collision momentum is described. The effect of the laser pulse intensity on the transitions from the continuum state to the bound vibrational states is discussed in detail. The photodissociation accompanied with photoassociation reaction is also described.

2. Theoretical treatment

The dynamic process of the photoassociation reaction $F(^2P)+H(^2S) \rightarrow HF(X^1\Sigma^+)$ can be described by the time-dependent Schrödinger equation

$$\mathrm{i}\hbar\frac{\partial}{\partial t}\Psi(r,t) = (\hat{H}_{\mathrm{mol}} + \hat{H}_{\mathrm{int}})\,\Psi(r). \tag{1}$$

Initially, at $t = 0$, the wavefunction with the coherent Gaussian type wave packet is given by

$$\Psi_0(r) = \Big(\frac{2}{\pi d_0}\Big)^{1/4}\exp\Big[\mathrm{i}k_{\mathrm{e}}r - \Big(\frac{r-r_{\mathrm{e}}}{d_0}\Big)^2\Big], \tag{2}$$

where the parameter d_0 denotes the width of the wave packet, and r_{e} is the average initial distance of the two atoms.

When F and H are close to each other, they can combine into a HF molecule. The molecular Hamiltonian is given by

$$\hat{H}_{\mathrm{mol}} = \frac{\hat{p}^2}{2m} + U(r), \tag{3}$$

with

$$U(r) = D_0\exp[-2\beta(r-r_0)] - 2\exp[-\beta(r-r_0)] - D_0, \tag{4}$$

where $m = 1744.63207m_{\mathrm{e}}$ (m_{e} is the electron rest mass) is the reduced mass of the HF molecule and $U(r)$ denotes the Morse potential. In Eq.(4), the well depth $D_0 = 0.225009E_{\mathrm{H}}$ and the Morse parameter

*Project supported by the National Natural Science Foundation of China (Grant Nos 10674022 and 20633070).
†Corresponding author. E-mail: shlcong@dlut.edu.cn

$\beta = 1.174014a_0^{-1}$, where $E_{\rm H}$ is the Hartree energy and a_0 is the Bohr radius.[29]

In Eq.(1), $\hat{H}_{\rm int}$ denotes the interaction of the molecule with the linearly polarized laser field. In the electric dipole moment approximation, the interaction Hamiltonian can be written as

$$\hat{H}_{\rm int} = -\mu(r)\varepsilon(t), \tag{5}$$

where $\mu(r)$ is the dipole moment of the HF molecule and $\varepsilon(t)$ represents the laser electric field. The molecular dipole moment function is given by[29]

$$\mu(r) = qr\exp(-\gamma r^4), \tag{6}$$

where $q = 0.454141$ e (e is the elementary charge), and $\gamma = 0.0064a_0^{-4}$. The dipole moment is shown in Fig.1(b).

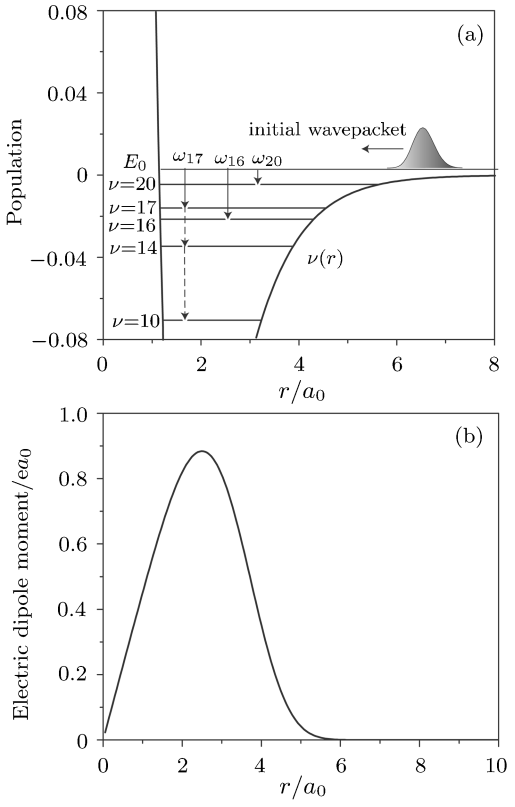


Fig.1. (a) The potential energy curve of HF molecule. (b) The electric dipole moment curve.

The electric field with a $\sin^2$t pulse shape is given by

$$\varepsilon(t) = \varepsilon_0 \sin^2\Big(\frac{\pi t}{\tau_{\rm p}}\Big)\cos(\omega_{\rm p} t), \tag{7}$$

where ε_0 is the electric field amplitude; $\tau_{\rm p}$ and $\omega_{\rm p}$ are the duration and the carrier frequency of the laser pulse, respectively.

In the interaction picture, the time-dependent wavefunction is composed of terms of the continuum state $|e\rangle$ and the bound state $|\nu\rangle$, and can be written as[20,24]

$$\Psi(r,t) = \Psi_\upsilon(r) + \Psi_{\rm e}(r,t), \tag{8}$$

with

$$\Psi_\upsilon(r) = \sum_{\nu=0}^{N-1} \lambda_\upsilon \exp(-{\rm i}E_\nu t/\hbar)|\nu\rangle \tag{9}$$

$$\Psi_{\rm e}(r,t) = \int d_{\rm e}\lambda_{\rm e}\exp(-{\rm i}E_{\rm e}t/\hbar)|e\rangle, \tag{10}$$

where E_ν is the vibrational level of the HF molecule, and $E_{\rm e}$ is the collision energy, λ_ν and $\lambda_{\rm e}$ are the expanding coefficients for the bound and continuum states, respectively. According to the expression[30,31]

$$N = \frac{2D_0}{\hbar\omega_\sigma} - 0.5, \tag{11}$$

one can obtain the maximal vibrational quantum number $N = 23$. The bound vibrational level is given by

$$E_\nu = \hbar\omega_\sigma(\nu + 0.5)[1 - \chi_{\rm e}(\nu + 0.5)] - D_0, \tag{12}$$

where $\omega_\sigma = \beta\sqrt{2D_0/m}$ and $\chi_\sigma = \hbar\omega_\sigma/4D_0$.

When the laser intensity is not very strong, the bound-bound transitions can be neglected. The expanding coefficient λ_ν can be expressed as[32]

$$\lambda_\nu = -\frac{\rm i}{\hbar}\lambda_0\langle\nu|\mu(r)|e\rangle\int_0^{\tau_{\rm p}} {\rm d}t'\varepsilon(t')\exp({\rm i}\omega_{\rm p}t'), \tag{13}$$

where $\lambda_0 = \lambda_{\rm e}(t = 0)$, $\omega_{\rm p}$=$(E_{\rm e} - E_\nu)/\hbar$ is the laser pulse carrier frequency.

The populations of the vibrational state $|\nu\rangle$ and all the bound vibrational states are calculated by $P_\nu = |\lambda_\nu|^2$ and $P_{\rm tot} = \sum_{\nu=0}^{N-1} P_\nu$, respectively. The selectivity of the bound vibrational state is described by the ratio $R = P_\nu/P_{\rm tot}$.

3. Results and discussions

In the photoassociation reaction, H+F→ HF, the laser pulse causes H and F atoms to form HF molecule via a transition from the continuum state $|e\rangle$ down to the bound vibrational state $|\nu\rangle$. The continuum state $|e\rangle$ and the bound vibrational state $|\nu\rangle$ correspond to the reagents H+F and the product HF, respectively. For a given initial collision momentum, the laser pulse parameters can be optimized. The laser pulse frequency is determined by $\omega_{\rm p}$=$(E_{\rm e} - E_\nu)/\hbar$. The optimal pulse duration $\tau_{\rm p}$ is approximately equal to the time of scattering process.[20,23] When the pulse frequency and duration are fixed, the pulse amplitude

can be adjusted until the final population of selective vibrational state reaches its maximal value.

We first study the laser-induced photoassociation transition from the continuum state $|e\rangle$ down to a selective vibrational state $|\nu = 16\rangle$. Figure 2 shows the final populations $P_{\nu=16}$ and $P_{\rm tot}$ versus $|k_{\rm e}|$. The curve of $P_{\nu=16}$ almost overlaps that of $P_{\rm tot}$, which means that there is no other transition to occur and the vibrational state-selectivity is highly efficient (nearly 100%). In the region of $|k_{\rm e}| = 0.5 - 3.0a_0^{-1}$, the two overlapped curves increase with the increase of $|k_{\rm e}|$. At $|k_{\rm e}| = 3.0a_0^{-1}$, the two curves reach their maximal values, and then decrease with the increase of $|k_{\rm e}|$.

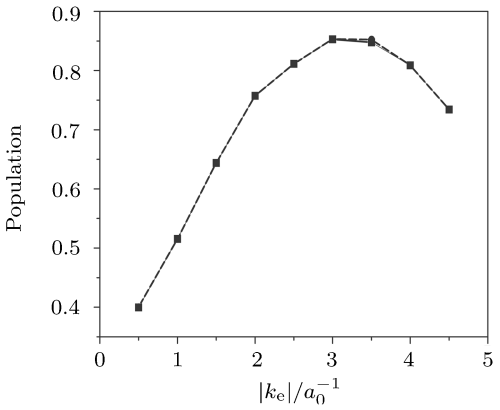


Fig.2. The populations $P_{\nu=16}$ (solid curve) and $P_{\rm tot}$ (dot curve) versus $|k_{\rm e}|$.

We then discuss the transitions from the continuum state down to the different vibrational states when the initial momentum is fixed at $|k_{\rm e}| = 3.0a_0^{-1}$. For each vibrational state, in order to obtain the maximal population, the laser intensity must be optimized. Figure 3 shows the evolutions of populations for $\nu = 16$, 15 and 14 vibrational levels with time. When $\nu = 16$, 15 and 14, the amplitudes of optimal laser pulses are $\varepsilon_0 = 19.532$, 25.186 and 51.914 GV/m, respectively. This shows that the stronger laser pulse can transfer the population of the continuum state to the lower vibrational level. This may be interpreted as follows. With the decrease of the vibrational quantum number ν, the dipole coupling matrix element $\langle\nu|\mu(r)|e\rangle$ in Eq.(13) decreases rapidly.[23] In order to obtain a larger population, we must increase the intensity (i.e., amplitude ε_0) of the laser pulse. We notice that, however, when the laser intensity is very strong, other transitions may occur. In Fig.3(c), there is a separation between the two curves $P_{\nu=14}$ and $P_{\rm tot}$. The separation indicates that the multiphoton transition and the dissociation process HF→H+F may take place along with the association reaction.

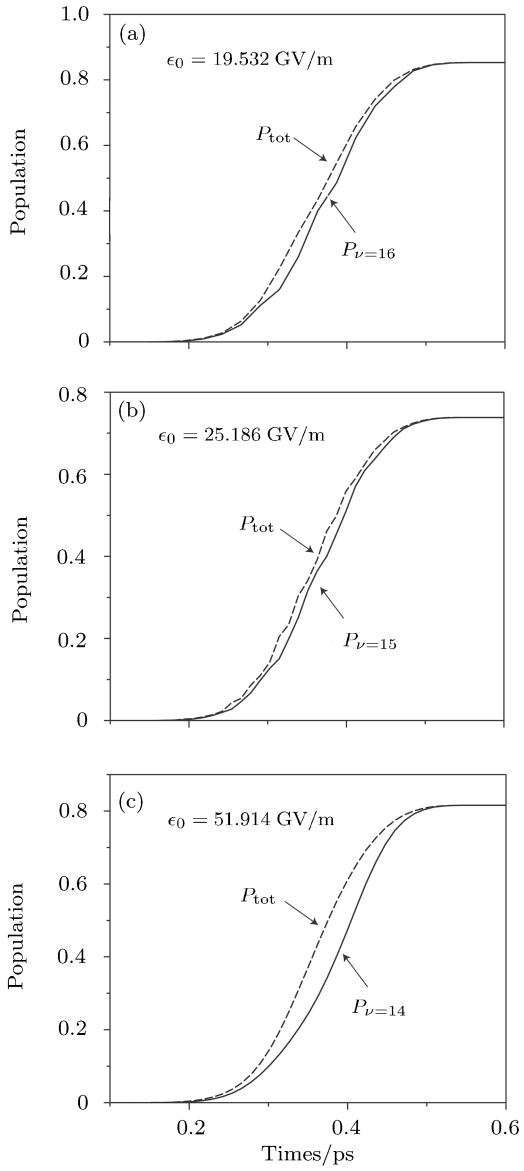


Fig.3. The population distributions of vibrational states $\nu = 16$, 15 and 14 for $|k_{\rm e}| = 3.0a_0^{-1}$. (a) $\nu = 16$ and $\varepsilon_0 = 19.532$ GV/m. (b) $\nu = 15$ and $\varepsilon_0 = 25.186$ GV/m. (c) $\nu = 14$ and $\varepsilon_0 = 51.914$ GV/m.

The multiphoton transitions are illustrated in Figs.1(a) and 4(a). When $|k_{\rm e}| = 3.0a_0^{-1}$ and $\varepsilon_0 = 17.99$ GV/m, the one-, two- and three-photon transitions take place from the continuum state to the bound vibrational levels $\nu = 17$, 14 and 10, as shown in Fig.1(a). The transition processes can be expressed as $|e\rangle \xrightarrow{\hbar\omega} |\nu = 17\rangle$, $|e\rangle \xrightarrow{2\hbar\omega} |\nu = 14\rangle$ and $|e\rangle \xrightarrow{3\hbar\omega} |\nu = 10\rangle$. In Fig.4(a), the maximal values of $P_{\nu=14}$ and $P_{\nu=10}$ appear at $t = 0.399$ and 0.387 ps, respectively. The ratios at $t = 0.399$ and 0.387 ps are $P_{\nu=14}/P_{\rm tot} = 20.55\%$ and $P_{\nu=10}/P_{\rm tot} = 6.34\%$, respectively. This indicates that when the laser pulse

carrier frequency satisfies the resonant transition condition, $(E_e - E_\nu)/\hbar = n(E_e - E_{\nu=17})/\hbar$ (where n is an integer), the multiphoton transitions will take place. Figure 4(b) shows the process of two-photon transition from the state $|e\rangle$ to the vibrational state $|\nu = 14\rangle$. The maximal multiphoton transition rate, $R_{\max}$, increases with the increase of the pulse amplitude (from $\varepsilon_0 = 5.14$ to 35.98 GV/m). This shows that the larger pulse amplitude can induce a higher probability of the multiphoton transition. In Fig.4(a), the $P_{\nu=14}$ and $P_{\nu=10}$ decrease with time after they reach the maximal values, and the final ratios are $P_{\nu=14}/P_{\rm tot} = 6.23\%$ and $P_{\nu=10}/P_{\rm tot} = 1.20\%$. It can be seen that the population of the vibrational states for $\nu = 14$ and 10 are very small when the pulse is over. Thus, except the dominating transition $|e\rangle \xrightarrow{\hbar\omega} |\nu = 17\rangle$, there exist other transition processes, including the bound → bound state transitions, $\nu = 17 \to 14$ and $\nu = 17 \to 10$, and bound → continuum state transition (dissociation process).

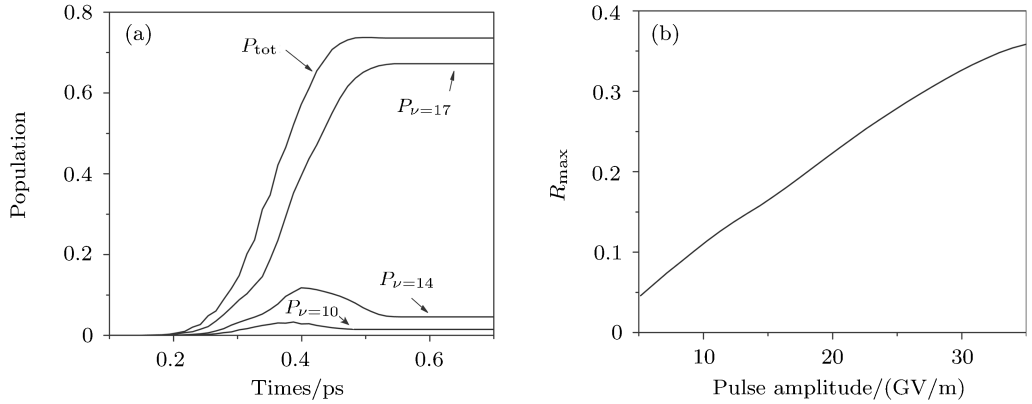


Fig.4. (a) Evolutions of populations of vibrational states with $\nu = 17$, 14 and 10 for $|k| = 3.0a_0^{-1}$ and $\varepsilon_0 = 17.99$ GV/m. (b) The maximal rate $R_{\max}$ of two-photon transition $|e\rangle \xrightarrow{2\hbar\omega} |\nu = 14\rangle$ versus the laser pulse amplitude.

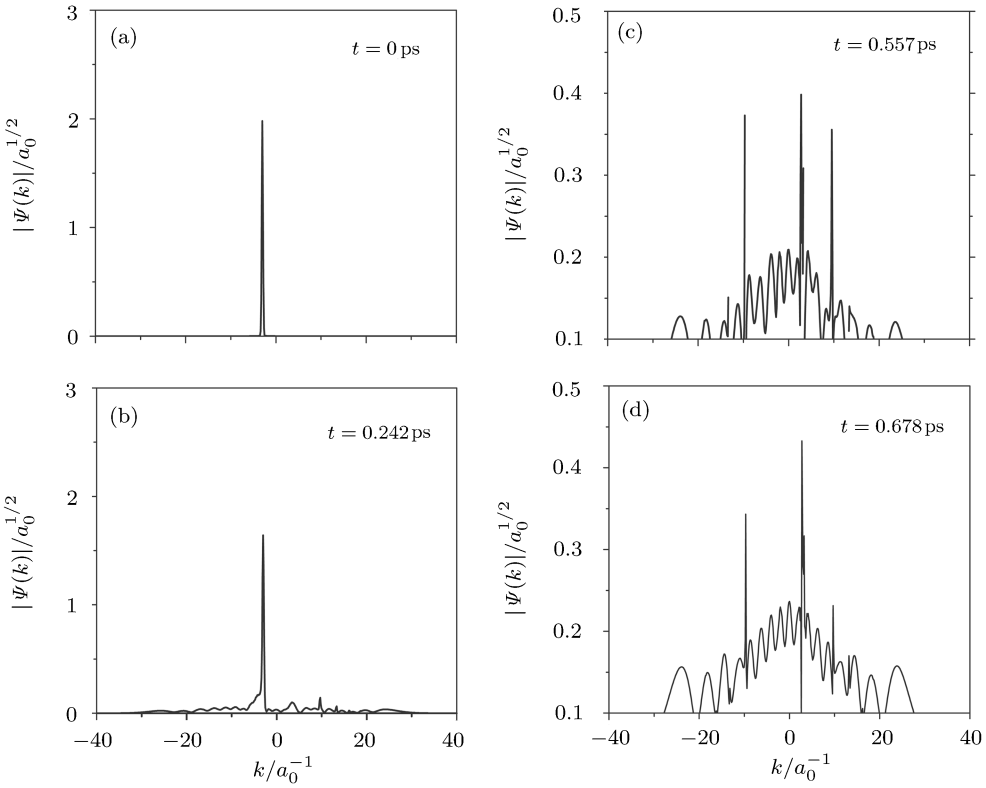


Fig.5. Evolutions of the wavepacket with $|k|$ at different times in the momentum space.

The dissociation process can be described in the momentum space. Figure 5 shows the wave packet dynamics in the momentum space representation at different times, where $\nu = 16$ and $|k_e| = 3.0a_0^{-1}$. It can be seen from Fig.5 that the peaks of initial wavefunction $|\Psi(k)|$ appear at $t = 0.242$, 0.557 and 0.678 ps. In the calculation, we find that the energy difference between two neighbouring peaks equals one-photon energy. These peaks indicate that the product HF of association reaction may be dissociated by the multiphoton absorption.

In the present work, we do not consider the practical linewidth of the driving laser pulse. In fact, with an ultrashort laser pulse, the linewidth (frequency spread) is quite large. Especially for the laser pulse with several optical cycles, the linewidth can be $100 - 200$ nm. The efficiency of the vibrational state-selectivity in the photoassociation reaction will be influenced to a certain extent. However, our work here is just an exploratory study to show that it is possible to control the photoassociation reaction H+F→HF with an ultrashort laser pulse. Thus, the conclusions drawn above are of certain practical meaning. In the future work, we will improve our model to study the effect of the linewidth of laser pulse on the photoassociation dynamics.

4. Conclusion

In summary, the photoassociation reaction H+F→ HF induced by the ultrashort laser pulse has been studied theoretically. For a given initial collision momentum, the laser pulse parameters are optimized in order to obtain the maximal selective vibrational population in the product HF. Using the optimal laser parameters, we can efficiently control the product HF molecule in a selective vibrational state $|\nu = 16\rangle$. A stronger laser pulse can transfer the population of the continuum state to the lower vibrational state. When the laser pulse carrier frequency meets the resonant transition condition and the laser intensity is very strong, the multiphoton transitions and dissociation process will take place along with the one-photon transition. The multiphoton transition rate increases with the increase of the pulse amplitude. Although we take a simple model, the results may serve as a guideline for controlling the product of photoassociation reaction.

References

[1] Sun Z G, Liu H P, Lou N Q and Cong S L 2003 *Chem. Phys. Lett.* **369** 374

[2] Stapelfeldt H, Sakai H, Constant E and Corkum P B 1997 *Phys. Rev. Lett.* **79** 2787

[3] Zhang L D, Wei J, Jiang Y Y, Fang L, Zhang S D, Guo W Y and Cai J Y 1998 *Chin. Phys.* **7** 271

[4] Niu D W, Li H Y, Luo X L, Liang F,Cheng S and Li A L 2006 *Chin. Phys.* **15** 1511

[5] Wickenhauser M, Tong X M, Arbó D G, Burgdörfer J and Lin C D 2006 *Phys. Rev.* A **74** 041402

[6] Li G X, Huang G M and Peng J S 1998 *Chin. Phys.* **7** 422

[7] Eramo R, Cavalier S, Fini L, Matera M and Dimauro L F 1997 *J. Phys.* B **30** 3789

[8] Faucher O, Hertz E, Lavorel B, Chaux R, Dreier T, Berger H and Charalambidis D 1999 *J. Phys.* B **32** 4485

[9] Sage J M, Sainis S, Bergeman T and DeMille D 2005 *Phys. Rev. Lett.* **94** 203001

[10] Fioretti A, Comparat D, Crubellier A, Dulieu O, Masnou-Seeuws F and Pillet P 1998 *Phys. Rev. Lett.* **80** 4402

[11] Machholm M, Giusti-Suzor A and Mies F H 1994 *Phys. Rev.* A **50** 5025

[12] Lett P D, Helmerson K, Phillips W D, Ratliff L P, Rolston S L and Wagshul M E 1993 *Phys. Rev. Lett.* **71** 2200

[13] Miller J D, Cline R A and Heinzen D J 1993 *Phys. Rev. Lett.* **71** 2204

[14] Yu J, Wang S M, Yuan K J and Cong S H 2006 *Chin. Phys.* **15** 1996

[15] Dai C J and Chen Z D 2001 *Chin. Phys.* **10** 403

[16] Zheng L, Wang C, Li S H, Liu B C, Ni G Q, Li R X and Xu Z Z 2006 *Chin. Phys.* **15** 697

[17] Marvet U and Dantus M 1995 *Chem. Phys. Lett.* **245** 393

[18] Vala J, Dulieu O, Masnou-Seeuws F, Pillet P and Kosloff R 2000 *Phys. Rev.* A **63** 013412

[19] Vatasescu M, Dulieu O, Kosloff R and Masnou-Seeuws F 2001 *Phys. Rev.* A **63** 033407

[20] Niu Y Y, Wang S M and Cong S L 2006 *Chem. Phys. Lett.* **428** 7

[21] Javanainen J and Matt M 1998 *Phys. Rev.* A **58** R789

[22] Matt M and Javanainen J 1999 *Phys. Rev.* A **60** 3174

[23] Korolkov M V, Manz J, Paramonov G K and Schmidt B 1996 *Chem. Phys. Lett.* **260** 604

[24] Backhaus P and Schmidt B 1996 *Chem. Phys.* **217** 131

[25] Korolkov M V and Schmidt B 1997 *Chem. Phys. Lett.* **272** 96

[26] Korolkov M V and Schmidt B 1998 *Chem. Phys.* **237** 123

[27] Backhaus P, Manz J and Schmidt B 1998 *J. Phys. Chem.* A **102** 4118

[28] Korolkov M V and Schmidt B 2002 *Chem. Phys. Lett.* **361** 432

[29] Andrianov I V and Paramonov G K 1998 *Phys. Rev.* A **59** 2134

[30] Manz J, Paramonov G K 1993 *J. Phys. Chem.* **97** 12625.

[31] Tran P 1999 *Phys. Rev.* A **59** 1444

[32] Backhaus P and Schmidt B 1997 *Chem. Phys.* **217** 131